

Cryogenic operation of a 24 GHz MMIC SiGe HBT medium power amplifier

This article has been downloaded from IOPscience. Please scroll down to see the full text article.

2010 Semicond. Sci. Technol. 25 125002

(<http://iopscience.iop.org/0268-1242/25/12/125002>)

View [the table of contents for this issue](#), or go to the [journal homepage](#) for more

Download details:

IP Address: 216.165.157.215

The article was downloaded on 04/11/2010 at 04:05

Please note that [terms and conditions apply](#).

Cryogenic operation of a 24 GHz MMIC SiGe HBT medium power amplifier

Guoxuan Qin^{1,4,5}, Ningyue Jiang^{1,4,6}, Jung-Hun Seo^{1,4}, Namki Cho^{1,4}, George E Ponchak², Daniel van der Weide¹, Pingxi Ma³, Scott Stetson³, Marco Racanelli³ and Zhenqiang Ma¹

¹ Department of Electrical and Computer Engineering, University of Wisconsin, Madison, WI 53706, USA

² NASA Glenn Research Center, Cleveland, OH 44135, USA

³ Jazz Semiconductor, Inc., Newport Beach, CA 92660, USA

E-mail: mazq@engr.wisc.edu

Received 8 September 2009, in final form 13 July 2010

Published 3 November 2010

Online at stacks.iop.org/SST/25/125002

Abstract

The performance of a SiGe heterojunction bipolar transistor (HBT) millimetre-wave power amplifier (PA) operating at cryogenic temperature was reported and analysed for the first time. A 24 GHz two-stage medium PA employing common-emitter and common-base SiGe power HBTs in the first and the second stage, respectively, showed a significant power gain increase at 77 K in comparison with that measured at room temperature. Detailed analyses indicate that cryogenic operation of SiGe HBT-based PAs mainly affects (improves) the performance of the SiGe HBTs in the circuits due to transconductance enhancement through magnified, favourable changes of SiGe bandgap due to cooling ($\Delta E_g/kT$) and minimized thermal effects, with little influence on the passive components of the circuits.

(Some figures in this article are in colour only in the electronic version)

1. Introduction

Due to the attractive combination of high speed, high integration level and low cost, SiGe heterojunction bipolar transistor (HBT) technology has become increasingly prevalent in commercial RF and microwave applications for the past two decades [1]. As of today, a number of millimetre (mm)-wave integrated circuits (ICs) employing SiGe HBTs have already been demonstrated [2–8]. Among these ICs, mm-wave power amplifiers (PAs) appear to be the most challenging circuit to be implemented with SiGe HBTs. On the other hand, owing to the smaller bandgap of SiGe and the feasibility of heavy doping in SiGe and Si, SiGe HBTs have been shown to be superior semiconductor devices suitable for cryogenic applications [9–12]. These demonstrations and studies, combined with the excellent properties of tolerance to radiation of these devices, clearly indicated the potential of SiGe HBTs for high-frequency

space applications. Yet, previous cryogenic studies on SiGe HBTs were only focused on discrete low-power, high-speed devices/circuits and logic circuits. The PA requires large-signal operation and impedance matching has more important influences than small-signal amplifiers (such as low-noise amplifiers). Additionally, thermal effects in PAs are a lot more severe than any small-signal circuits. However, there have not been reports on the cryogenic operation of PA ICs that employ SiGe HBTs as their active devices. As a result, it has not been clear how cryogenic operation affects the entire PA circuits that employ both SiGe HBTs and passive components. In this paper, we report the performance of a two-stage, 24 GHz SiGe HBT-based medium-power PA operating at cryogenic temperature with the major focus on analysing how cryogenic operation influences the active and passive components in a mm-wave circuit.

2. Design of a SiGe HBT PA

Jazz Semiconductor's 0.18 μm SiGe90 process [13] was employed for the design and fabrication of the 24 GHz MMIC

⁴ These authors contributed equally.

⁵ Present address: Department of Electronic Science and Technology, Tianjin University, Tianjin, P. R. China.

⁶ Present address: Avago Technologies, San Jose, CA, USA.

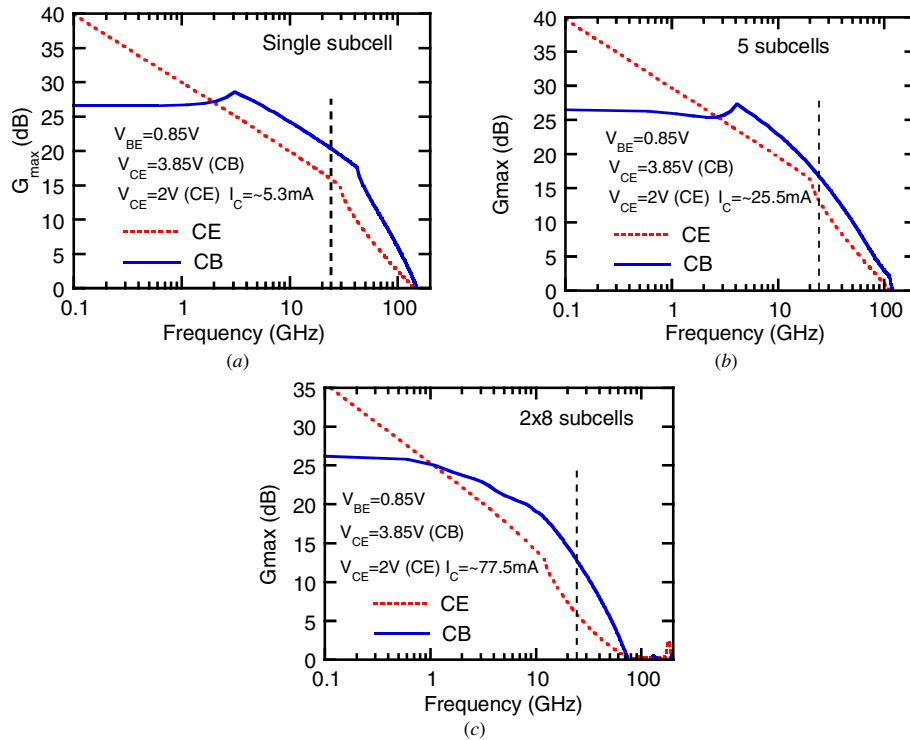


Figure 1. Simulated CE and CB power gain characteristics of (a) single SiGe HBT subcell (four emitter fingers), (b) 5 subcells and (c) 16 power subcells, with interconnect parasitics included (room temperature). $V_{BE} = 0.85$ V, $V_{CE} = 3.85$ V for CB and $V_{CE} = 2$ V for CE. $I_C = 5.3$, 25.5 and 77.5 mA for single subcell, 5 subcells and 16 subcells, respectively.

SiGe PA. SiGe HBTs with 80 GHz f_T , 190 GHz f_{max} , 3.5 V BV_{CEO} and 12.5 V BV_{CBO} were employed to provide high f_{max} while maintaining a sufficient bias margin. Five and 16 subcells were used in the first and the second stage of the PA, respectively. Each subcell contains four emitter fingers with dimensions of $0.2 \times 10.16 \mu\text{m}^2$ for each finger. The device area ratio of $\sim 1:3$ (5:16) for the two stages is chosen to provide adequate drive power from the first stage [2]. In the first stage, the common-emitter (CE) configuration was used. The common-base (CB) configuration was used in the second stage. Although some published SiGe HBT PA circuits already used the CB configuration for its available higher bias voltage than that of CE [2], the use of CB in this design was mainly based on the power gain considerations.

Previously we have demonstrated that CB SiGe HBTs always provide higher power gain than CE SiGe HBTs in a high frequency regime [14–16]. The CB superiority of power gain versus CE is also proved in this PA design. Figure 1(a) shows the comparison of simulated power gain of a single SiGe HBT subcell (4 emitter fingers). It is clear that, under equivalent bias conditions (i.e. the same collector current I_C), the CB configuration shows significantly higher power gain than that of the CE configuration in the high frequency regime (above ~ 2 GHz, ~ 4.5 dB more at 24 GHz). As the subcell number increases, power gain degradation is expected due to the increase of interconnect parasitics [17]. To further compare the power gain characteristics between the CE and CB configurations, 5 subcells and 16 subcells were simulated and the results are shown in figures 1(b) and (c), respectively. As can be seen, while the gain of these larger power cells

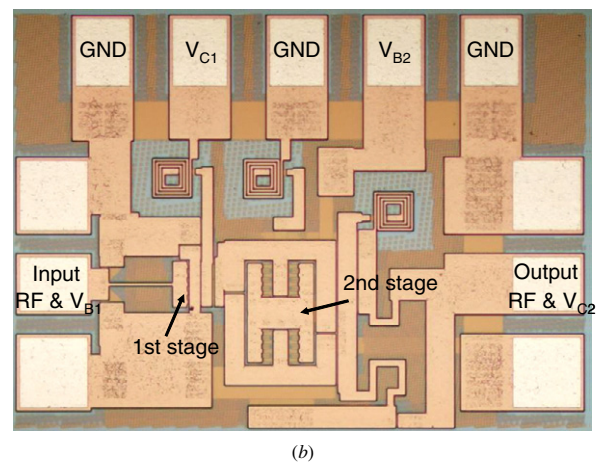
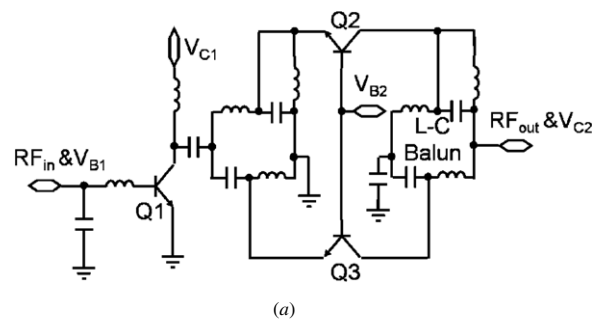


Figure 2. (a) Circuit diagram of the 24 GHz SiGe HBT PA. Q1 has five subcells. Q2 and Q3 are identical, each containing eight subcells. Bias conditions (RT): $V_{B1} = V_{B2} = 0.85$ V, $V_{C1} = 2$ V, $V_{C2} = 3.85$ V. (b) Microscopic image of the 24 GHz MMIC SiGe PA.

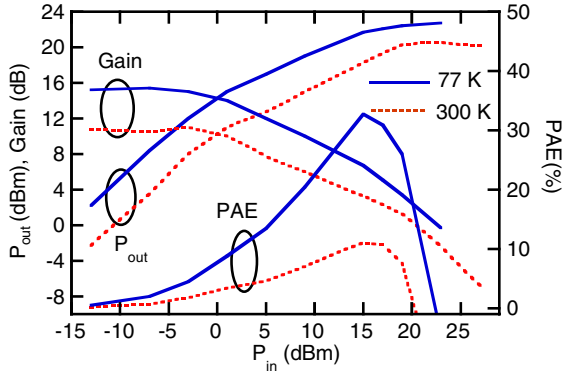


Figure 3. Comparison of measured large-signal power performance characteristics of the 24 GHz PA at RT and 77 K.

did degrade with respect to the single subcell (figures 1(a)), especially in the high frequency range, higher power gain can still be obtained from CB than from the CE configuration. As a result, CB should be a better choice for both gain stages. However, considering the small power gain difference (figure 1(b)) between CE and CB for the five subcells, the ease of matching circuit design and simplicity of bias, we used the CE configuration for the first stage. Since the second stage will need to be biased at higher levels than the first stage and the power gain of the CB configuration is ~ 7 dB higher than the CE configuration, we adopted CB for the second stage. In order to obtain better virtual RF ground for the CB configuration, differential topology and on-chip baluns were used [2, 18, 19] for the second stage. Impedance matching for the CB stage was also achieved with the baluns. In this study, the major goal was to investigate the cryogenic operation mechanism of PAs, i.e. how cryogenic operation influences the active and passive components in a mm-wave circuit, instead of realizing a new power performance record. To simplify the analysis, no third stage was implemented in the PA circuit. Figures 2(a) and (b) show the microscopic image and the circuit diagram of the SiGe HBT PA, respectively.

3. Measurement results and analysis

On-wafer GSG probing measurements were conducted for both small- and large-signal characteristics of the PA at room temperature (RT, 300 K) and 77 K. To maintain accuracy for these measurements, shot-open-load-thru (SOLT) calibrations were carried out at the respective (RT and cryogenic) temperatures. The designed operation frequency (24 GHz) lies in the unconditional stable frequency range of both SiGe (5 and 16) subcells, as indicated in figure 1. The PA is stable, even though its input was not perfectly impedance matched at certain frequencies. The linearity characteristics of the PA were also measured at RT and 77 K with two-tone measurements and 10 MHz frequency spacing.

As shown in figure 3, the two-stage MMIC SiGe PA exhibited 20.6 dBm output power (P_{out}) at 24 GHz with 11 dB power gain, and the peak power-added efficiency (PAE) is 11% at RT. The power performance of the PA is greatly enhanced at 77 K. The P_{out} is 22.7 dBm with a power gain of 15.4 dB and 32.7% peak PAE.

The small-signal characteristics of the SiGe PA were also characterized at cryogenic temperatures (77 K and 187 K), with the same dc current as RT maintained. Figure 4(a) plots the comparison of the measured small-signal power gain (S_{21}) of the circuit, under equivalent output dc current at different temperatures, for the frequency range of 20 to 30 GHz. At 24 GHz, the PA exhibited 16.5 dB and 20.0 dB at RT and 77 K, respectively. The S_{21} enhancement is 3.5 dB. In figure 4(b), the PA matching conditions (S_{11} and S_{22}) that were simultaneously measured were compared between RT and the cryogenic temperatures. Although the input matching point of the circuit was slightly off the designed frequency 24 GHz, which results in a poor return loss at the operation frequency, figure 4(b) clearly indicates that negligible changes in the input and output impedance of the PA circuit were observed. These results clearly demonstrate that high-frequency SiGe HBT PAs are excellent contenders for cryogenic applications.

Figure 5 shows the measured linearity characteristics of the PA at 24 GHz. As shown in the figure, the input/output third-order intercept points (IIP3/OIP3) at 77 K and RT are $-0.4/16.0$ dBm and $3.6/17.0$ dBm, respectively.

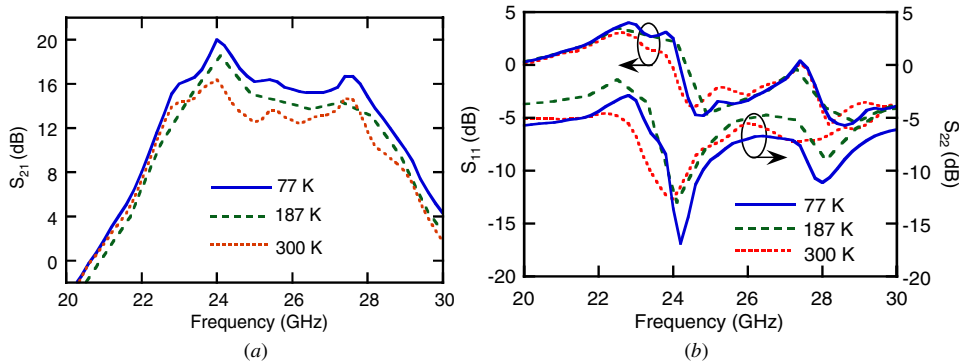


Figure 4. Comparisons of measured S-parameters of the 24 GHz PA at RT and cryogenic temperatures (187 K, 77 K). (a) Small-signal power gain S_{21} . (b) Input matching S_{11} and output matching S_{22} . The bias voltages are the same as that listed in the caption to figure 2, except for that $V_{B1} = V_{B2} = 0.87$ V at 77 K.

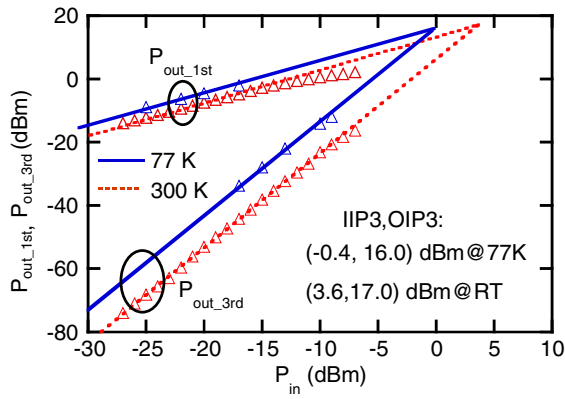


Figure 5. Comparison of the measured linearity characteristics of the 24 GHz PA at RT and 77 K. The dashed lines are used to guide the data view.

The third-order output power (P_{out_3rd}) of the PA dramatically increased with the decrease of temperature, while the first-order output power (P_{out_1st}) slightly increased. As indicated, for the measured frequency range, the linearity of the PA at RT is slightly better than that at 77 K.

Based on the fact that the impedance matching conditions have almost no change as indicated in figure 3(b), we speculate that the passive components used in the PAs are not significantly influenced by cryogenic temperatures. Instead, the dramatic performance enhancement of the PA is believed to be mainly due to the transconductance enhancement of the SiGe HBTs through the magnified favourable changes of the SiGe bandgap due to cooling ($\Delta E_g/kT$). In order to

verify the above hypothesis, ADS simulations were conducted to analyse the power gain (S_{21}) characteristics for each of the two stages at both RT and cryogenic temperatures. Figures 6(a) and (b) show the S_{21} comparisons for the SiGe HBT power cells in both the first and the second stages (interconnect parasitics effects included) between RT and 77 K, respectively. Under equivalent output current, the first/second stages exhibit 1.70/1.61 dB higher power gain at 24 GHz at cryogenic temperature than at the RT. The S_{21} of the entire circuit with matching circuits included was also simulated and the results are consistent with that shown in figure 6(a) and (b), as shown in figure 6(c). The total power gain improvement from the simulations is 3.31 dB. Apparently, the power gain improvement contributed by the two SiGe power HBTs at cryogenic temperature closely matched with the total measured power performance enhancement (3.5 dB). The slight difference (0.19 dB = 1.04: 4% difference) could be attributed to the minimized thermal effects under cryogenic operation because of the much better heat dissipation conditions, as well as partially due to measurement inaccuracy (varied from circuits to circuits). Based on our observations from the measurements, both stages experienced self-heating during operation at RT (note that the PA chips need to sit on the metal stage of the probe station to avoid thermal runaway during operation and they can melt a plastic substrate if mounted so) due to the large device size, and the self-heating should have increased the junction temperatures for the two power cells. The self-heating is particularly observed at higher bias levels. However, we did not observe such self-heating when the PA was operated at

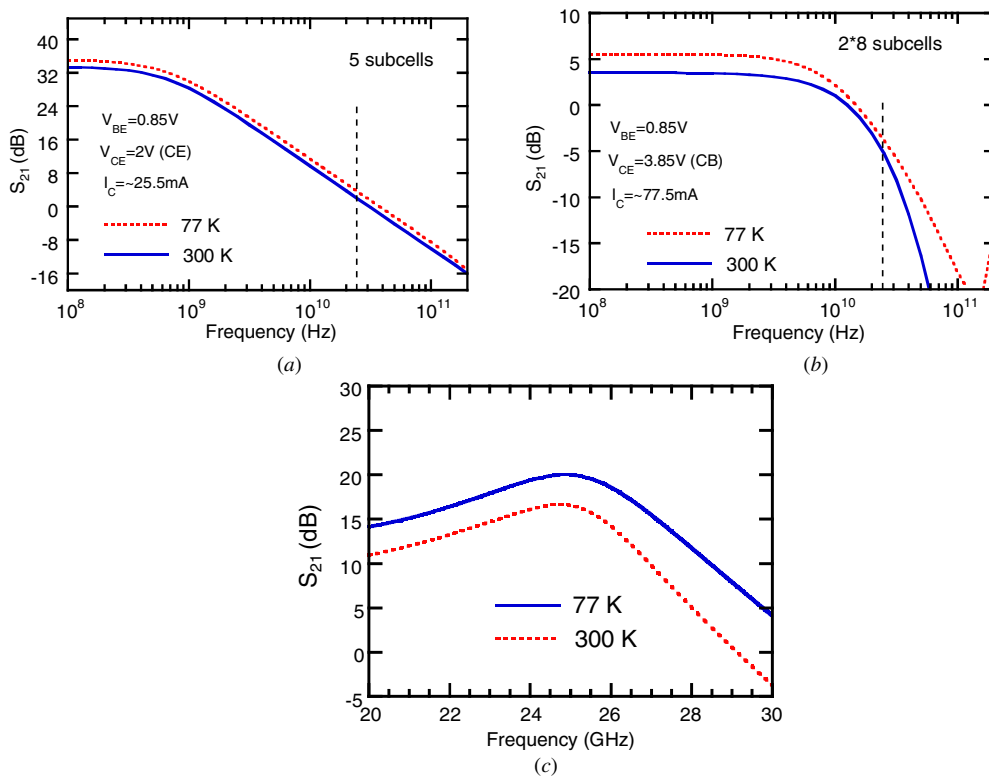


Figure 6. Simulated power gain (S_{21}) characteristics of: (a) first stage, (b) second stage and (c) the entire circuit at RT and 77 K.

cryogenic temperatures, even though a plastic substrate was used. The self-heating at RT could have increased the junction temperatures for the two power cells.

It is believed that the cryogenic operation has also caused the total parasitic input (first stage) resistance (base-emitter resistance: $R_{BE} = R_B + R_E = R_{B,semi} + R_{B,metal} + R_{E,semi} + R_{E,metal}$) increase and the increase of the base-to-ground resistance of the second stage, which is indicated by the small increase of bias voltages (e.g., $V_{B1} = V_{B2} = 0.87$ V at 77 K versus 0.85 V at RT) applied to the circuit while maintaining the same bias current levels as for the RT. The total parasitic resistances at both stages include metal resistance and semiconductor resistance. At cryogenic temperatures, metal resistance decreases and semiconductor resistance increases. For the first stage (only five subcells), the base semiconductor resistance ($R_{B,semi}$) is much higher than the base metal resistance ($R_{B,metal}$), while the emitter semiconductor resistance ($R_{E,semi}$) could be comparable with or even lower than the emitter metal resistance ($R_{E,metal}$). As a result, based on the measured bias change, the input resistance (R_{BE}) increase is caused by the increase of total base resistance (R_B), in which the base semiconductor resistance ($R_{B,semi}$) dominates. The emitter resistance change (R_E) is reflected on the slight changes of the linearity characteristics (figure 5). Higher emitter resistance resulted in higher IIP3/OIP3 [20]. Therefore, the total emitter parasitic resistance (R_E) is very slightly decreased, in which the emitter metal resistance dominates at 77 K. Based on simulations, the total base resistance change is about 18 Ω . However, combining with the inductor and capacitor used for the input matching circuit, such a resistance change was still not sufficiently large to cause any substantial changes for the impedance matching.

4. Conclusion

Performance of a two-stage 24 GHz SiGe HBT medium PA operating at cryogenic temperature was reported and analysed in this paper. The two-stage PA employing common-emitter and common-base SiGe power HBTs in the first and the second stage, respectively, exhibited a nearly 3.5 dB power gain increase at liquid nitrogen temperature than room temperature (RT). The linearity characteristics were slightly degraded at 77 K. Both experimental and simulation results indicate that cryogenic operation of SiGe HBT-based PAs only affects (improves) the performance of the active components of the circuits, while the influence on the passive components is not sufficient to affect the impedance matching of the circuits.

As a result, not only are discrete SiGe HBTs a contender for cryogenic electronics applications, but also the ICs employing these high-speed devices.

Acknowledgment

The authors acknowledge the fabrication support of the processing team at Jazz Semiconductor.

References

- [1] Rieh J S et al 2004 *IEEE Trans. Microw. Theory Tech.* **52** 2390
- [2] Cheung T S D and Long J R 2005 *IEEE J. Solid-State Circuits* **40** 2583
- [3] Komijani A and Hajimiri A 2006 *IEEE J. Solid-State Circuits* **41** 1749
- [4] Floyd B A, Reynolds S K, Pfeiffer U R, Zwick T, Beukema T and Gaucher B 2005 *IEEE J. Solid-State Circuits* **40** 156
- [5] Pfeiffer U R, Reynolds S K and Floyd B A 2004 *IEEE Radio Frequency Integrated Circuits (RFIC) Symp. (Fort Worth, TX, June 6–8, 2004)* p 91
- [6] Welch B and Pfeiffer U 2006 *IEEE Radio Frequency Integrated Circuits (RFIC) Symp. (San Francisco, CA, June 11–13, 2006)* p 4
- [7] Kinayman N, Jenkins A, Helms D and Gresham I 2005 *IEEE Radio Frequency Integrated Circuits (RFIC) Symp. (Long Beach, CA, June 12–14, 2005)* p 91
- [8] Joseph A J et al 2003 *IEEE J. Solid-State Circuits* **38** 1471
- [9] Cressler J D, Comfort J H, Crabbe E F, Patton G L, Lee W, Sun J, Stork J M C and Meyerson B S 1991 *IEEE Electr. Dev. Lett.* **12** 166
- [10] Crabbe E F, Patton G L, Stork J M C, Comfort J H, Meyerson B S and Sun J Y C 1990 *Tech. Digest IEEE Int. Electr. Dev. Meeting (San Francisco, CA, December 9–12, 1990)* p 17
- [11] Cressler J D, Comfort J H, Crabbe E F, Patton G L, Stork J M C, Sun J Y C and Meyerson B S 1993 *IEEE Trans. Electr. Dev.* **40** 525
- [12] Hsieh M W, Hsin Y M, Liang K H, Chan Y J and Tang D 2006 *IEEE Trans. Electr. Dev.* **53** 1452
- [13] http://www.jazzsemi.com/process_technologies/sige.shtml
- [14] Ma Z and Jiang N 2005 *IEEE Trans. Electr. Dev.* **52** 248
- [15] Wang G, Yuan H C and Ma Z 2006 *IEEE Electr. Dev. Lett.* **27** 371
- [16] Ma Z and Jiang N 2006 *IEEE Trans. Electr. Dev.* **53** 875
- [17] Jiang N, Ma Z, Ma P and Racanelli M 2007 *Proc. EuMC (Munich, Germany, October 8–12, 2007)* 150
- [18] Simburger W, Wohlmuth H D, Weger P and Heinz A 1999 *IEEE J. Solid-State Circuits* **34** 1881
- [19] Bakalski W, Simburger W, Thuringer R, Wohlmuth H D and Scholtz A L 2003 *IEEE MTT-S Int. Microwave Symp. Digest (Philadelphia, PA, June 8–13, 2003)* vol 2 p 695
- [20] Yuan X et al 2002 *Proc. 3rd Int. Conf. on Microwave and Millimeter Wave Technology (Beijing, China, August 17–19, 2002)* p 70